J. Fluid Mech. (1989), *vol.* 206, *pp.* 545–561
Printed in Great Britain

Stabilization of dielectric liquid bridges by electric fields in the absence of gravity

By H. GONZÁLEZ[1], F. M. J. McCLUSKEY[2], A. CASTELLANOS[1] AND A. BARRERO[3]

[1] Dpto Electrónica y Electromagnetismo, Universidad de Sevilla, Spain
[2] Dpto Física Fundamental, U.N.E.D. Madrid, Spain
[3] Dpto de Ingeniería Energética y Mecánica de Fluidos, Universidad de Sevilla, Spain

(Received 25 July 1988 and in revised form 14 March 1989)

The stability of liquid bridges in zero gravity conditions under the influence of an a.c. electric field tangential to the interface is examined in this paper. For the theoretical study, a static analysis was carried out to find the bifurcation surfaces as a function of the three relevant non-dimensional parameters: Λ, the slenderness or ratio of height to diameter of the cylindrical bridge; β_0, the ratio of dielectric constants of the two fluids used and Ξ, a non-dimensional quantity proportional to the applied voltage. Stable and unstable regions of Λ–β_0–Ξ space were distinguished. Results indicate a strong stabilizing effect for higher values of β_0. The experimental study, using silicone and ricinus oil to approximate zero gravity conditions fully confirmed quantitatively the theoretical results.

1. Introduction

There has for a long time been an interest in the behaviour of liquids under the influence of gravity and capillary forces, and subjected to electric fields. These studies were primarily motivated by numerous industrial applications, e.g. electrostatic paint spraying, image making, ink matrix printers, electrohydrodynamic mixing, propulsion, heat transfer. A second motivation for such studies was the need to understand and control the location and motion of liquids, particularly of liquid propellants, in orbiting vehicles. The geometrical configurations usually considered for the liquid in such cases were flat interfaces, fluid jets or isolated drops. It is outside the scope of this paper to attempt to cover the extensive literature on these subjects, since most of the work is concerned with semi-insulating or conducting liquids. Our aim is to point out some of the relatively few works dedicated to purely dielectric liquids, at least as an admissible limit, subjected to tangential electrical fields at the interface (see Nayyar & Murty 1960; Melcher 1963; Melcher & Hurwitz 1967; Melcher & Schwartz 1968; Rosenkilde 1969; Saville 1970; Miksis 1981; Cheng & Chaddock 1984).

Recently, there has been renewed interest in the confinement of liquids by surface tension, in order to examine the possibilities of avoiding contact between a liquid and a containing vessel for applications to material processing. For example, the floating zone technique (Hurle, Müller & Nitsche 1987) has been successfully applied to grow high-quality crystals of different electronic materials (e.g. Si, CdTe, GaSb, InP). In this technique a container-free floating zone is established, by melting, in the sample rod to be processed. From the mechanical point of view, this floating zone can be

modelled as a liquid bridge, i.e. a body of fluid anchored between coaxial circular disks. In these applications it is desirable to have a liquid bridge as large as possible with the liquid flow kept to a minimum. Unfortunately these liquid bridges can become unstable owing to the effects of surface tension (Martínez, Haynes & Langbein 1987) in the same way as liquid jets. Moreover, previous theoretical and experimental results have shown that these liquid bridges are subjected to instabilities due to variations in surface tension induced by thermal gradients, residual gravity, rotations, axial accelerations, value of the contact angle, etc. (see Hurle *et al.* 1987 and references therein). The real situation is extremely complex and, therefore, to understand the underlying physics it is necessary to consider more simple specific phenomena, both theoretically and experimentally.

Here we study the effect of an a.c. electric field upon the stability of a liquid cylindrical bridge in the absence of gravity and thermal gradients. The motivation to consider electric fields stems from the well-known fact that for an insulating liquid jet both the critical wavenumber at which instability sets in and the initial growth rate of the most unstable disturbance decrease as the electric field strength increases. To minimize the gravity effects, theoretically as well as experimentally, we surround the liquid bridge with another liquid of the same density, in the so-called Plateau tank.

The paper is organized as follows. In the first part we formulate the problem and perform the stability analysis. In the second part we describe the experimental set-up and compare the experimental results to the theoretical ones.

2. Formulation of the problem

Consider the physical situation shown schematically in figure 1. The inner (i) and outer (o) liquids are assumed to be immiscible and of the same density. If liquid i is anchored between two bounding plates of equal radius, then for an appropriate value of its volume, this liquid will form a perfectly cylindrical column, i.e. a cylindrical liquid bridge, under the sole action of the surface tension forces at the interface of the two liquids. When an a.c. or d.c. potential difference is applied to the bounding plates (electrodes) new forces will act upon the liquids. For highly insulating liquids, where the electrical currents are very small, magnetic effects are negligible, and any such forces can be disregarded. We are then left with forces of electrical origin only given by (see Landau & Lifshitz 1971):

$$(\boldsymbol{F}_V)_e = \rho_e \boldsymbol{E} - \tfrac{1}{2}E^2\nabla\epsilon + \tfrac{1}{2}\nabla\left[\rho\left(\frac{\mathrm{d}\epsilon}{\mathrm{d}\rho}\right)_T E^2\right], \tag{1}$$

where ρ_e is the free charge density; $\boldsymbol{E}$ the electric field; ϵ the electrical permittivity and ρ the mass density. Let us examine closely the three terms on the right-hand side of (1). The first term, $\rho_e \boldsymbol{E}$, is a Coulombian-type force. In general, the free charge density ρ_e will always be present even for highly insulating liquids, owing to dissociation of impurities or of the liquid itself, and the inevitable electrochemical reactions at the metal-electrode/liquid interface. These last are of paramount importance for electric field values of over a few kilovolts per centimetre (Denat, Gosse & Gosse 1979). The dynamics of the liquid will be strongly affected by this Coulomb-type force unless the charge carriers do not displace significantly. This will be the case if we apply an a.c. electric field with a period much shorter than the typical relaxation time of any of the liquids involved in the experiments. Fortunately, industrial frequency (50 Hz) is high enough that we may disregard this term for the

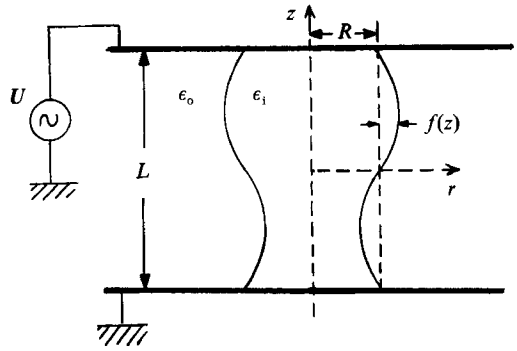

FIGURE 1. Schematic of bridge, indicating some relevant parameters.

vast majority of insulating liquids compared with the next term in (1). However, the melts of practical interest are typically good enough ionic conductors, owing to their relatively high temperature, and the frequency required must be high enough to satisfy the above condition. The second term, called the dielectrophoretic force, will be important whenever an inhomogeneous dielectric liquid is subject to an electrical stress. Here, it acts at the interface and normally to it. Therefore, this allows us to maintain the cylindrical shape as an equilibrium configuration in the presence of the imposed r.m.s. electric potential difference U. As this is not a volume force we need not retain this term in (1).

The third term, called electrostriction, acts both on the liquid bulk and at the interface. This electrostrictive force, being a pure gradient in the liquid bulk, is irrelevant to the dynamics of the liquids, since they are both assumed from the outset to be incompressible. Contrary to the usual convention of neglecting its contribution it may be convenient to see how it is cancelled through the corresponding term at the interface. Consequently, the Navier–Stokes equation which governs the liquid motion is

$$\rho\frac{\partial \boldsymbol{v}}{\partial t}+\rho\boldsymbol{v}\cdot\boldsymbol{\nabla}\boldsymbol{v}=-\boldsymbol{\nabla}p+\mu\nabla^2\boldsymbol{v}+\rho\boldsymbol{g}+\tfrac{1}{2}\epsilon b\boldsymbol{\nabla}(E^2),$$

where $\boldsymbol{v}$ is the velocity; p the pressure; $\boldsymbol{g}$ is the gravitational acceleration; μ the viscosity; b, defined as $\rho(\mathrm{d}\epsilon/\mathrm{d}\rho)_T/\epsilon$, is the electrostriction parameter, and E the modulus of the r.m.s. electric field.

The Navier–Stokes equation under hydrostatic conditions becomes a balance between volume and pressure forces:

$$\rho\boldsymbol{g}+\tfrac{1}{2}\epsilon b\boldsymbol{\nabla}(E^2)-\boldsymbol{\nabla}p=0. \tag{2}$$

This equation may be integrated and written as

$$p-\rho gz-\tfrac{1}{2}\epsilon bE^2=\Pi\equiv\text{constant}. \tag{3}$$

The effective pressure Π is different for each liquid, whereas the gravity term is the same for both since the densities are equal.

To the mechanical equations we must add the Maxwell equations which, for perfect dielectric liquids with zero conductivity and zero free charge density ($\rho_e=0$), reduce to the divergence and curl of the electric field, being both zero. Introducing in the usual way the electrical potential, this will have to satisfy the Laplace equation in each of the regions occupied by the liquids:

$$\nabla^2\Phi=0. \tag{4}$$

To complete the formulation of the problem, we must define the surface geometry and supplement the electromechanical equations with the corresponding boundary conditions. The interface is represented by the expression

$$F(r,\theta,z) \equiv r - f(\theta,z) = 0,$$

for which the outward normal vector is written

$$\boldsymbol{n} = \frac{\boldsymbol{\nabla} F}{|\boldsymbol{\nabla} F|} = \frac{1}{N(\boldsymbol{r})}\left(1, -\frac{1}{f}\frac{\partial f}{\partial \theta}, -\frac{\partial f}{\partial z}\right),$$

where

$$N(\boldsymbol{r}) \equiv \left[1 + \frac{1}{r^2}\left(\frac{\partial f}{\partial \theta}\right)^2 + \left(\frac{\partial f}{\partial z}\right)^2\right]^{\frac{1}{2}} \quad (\neq 0).$$

The relevant boundary conditions for our configuration are

(i) At the electrodes:

the voltage is fixed and the bridge is anchored:

$$\Phi(r,\theta,\tfrac{1}{2}L) = U, \quad \Phi(r,\theta,-\tfrac{1}{2}L) = 0, \tag{5}$$

$$f(\theta, \pm\tfrac{1}{2}L) = R. \tag{6}$$

(ii) On the interface:

(*a*) the tangential components of the electric field are equal at the interface or, equivalently, the electrical potential is continuous across it:

$$[\Delta\Phi]_{r=f} = 0. \tag{7}$$

The Δ notation represents the difference in a quantity as we cross the interface, $\Delta X = X_o - X_i$, where subscripts refer to outer and inner liquids respectively.

(*b*) the normal components of the electrical displacement vector $\epsilon \boldsymbol{E}$ are equal since we assume that there is no superficial charge on the interface:

$$\boldsymbol{n}\cdot[\Delta(\epsilon \boldsymbol{E})]_{r=f} = 0. \tag{8}$$

(*c*) the forces are in equilibrium at the interface:

$$\boldsymbol{n}[\Delta p \boldsymbol{I} - \Delta \boldsymbol{T}]_{r=f} = 0. \tag{9}$$

Here $\boldsymbol{I}$ is the unit tensor and $\Delta \boldsymbol{T}$ is the stress tensor jump across the interface, defined as

$$\Delta \boldsymbol{T} \equiv \Delta[\epsilon \boldsymbol{E}\boldsymbol{E} - \tfrac{1}{2}\epsilon(1-b)E^2\boldsymbol{I}] - \sigma \boldsymbol{\nabla}\cdot\boldsymbol{n}\boldsymbol{I},$$

where $\boldsymbol{E}\boldsymbol{E}$ is the diadic product of the electric field with itself, and σ is the superficial tension. The divergence of the normal vector to the interface has the form (see for example Struik 1957)

$$\boldsymbol{\nabla}\cdot\boldsymbol{n} \equiv -\frac{f\left[1+\left(\frac{\partial f}{\partial z}\right)^2\right]\left[\frac{\partial^2 f}{\partial \theta^2} - f\right] + f\frac{\partial^2 f}{\partial z^2}\left[f^2 + \left(\frac{\partial f}{\partial \theta}\right)^2\right] - 2\frac{\partial f}{\partial \theta}\left(\frac{\partial f}{\partial \theta} + f\frac{\partial f}{\partial z}\frac{\partial^2 f}{\partial \theta\,\partial z}\right)}{\left\{f^2\left[1+\left(\frac{\partial f}{\partial z}\right)^2\right] + \left(\frac{\partial f}{\partial \theta}\right)^2\right\}^{\frac{3}{2}}}.$$

We remark that the stress tensor jump comprises an electrical component (the Maxwell stress tensor) and a superficial tension one. Gravity does not appear obviously because it is a volume force. If we substitute p, given by (3), into (9), its radial component is now written:

$$\Delta\Pi+\sigma\nabla\cdot\boldsymbol{n}-\tfrac{1}{2}\Delta\left\{\epsilon\left[\left(\frac{\partial\Phi}{\partial r}\right)^2-\frac{1}{r^2}\left(\frac{\partial\Phi}{\partial\theta}\right)^2-\left(\frac{\partial\Phi}{\partial z}\right)^2\right]\right\}$$
$$+\frac{1}{r^2}\frac{\partial f}{\partial\theta}\Delta\left(\epsilon\frac{\partial\Phi}{\partial r}\frac{\partial\Phi}{\partial\theta}\right)+\frac{\partial f}{\partial z}\Delta\left(\epsilon\frac{\partial\Phi}{\partial r}\frac{\partial\Phi}{\partial z}\right)=0 \quad \text{at} \quad r=f. \tag{10}$$

It may be shown that the azimuthal and axial components of (9) are not independent of the radial component and the electrical conditions. They thus give no new information.

(iii) The electric field is finite on the axis $r = 0$, and uniform at large distances from the bridge. The potential therefore has the form

$$\Phi(0,\theta,z)=\text{finite}, \quad \Phi(\infty,\theta,z)=\frac{U}{L}(z+\tfrac{1}{2}L). \tag{11}$$

(iv) Finally we include a condition of constant volume for the bridge:

$$\frac{1}{2}\int_{-\frac{1}{2}L}^{\frac{1}{2}L}\mathrm{d}z\int_0^{2\pi}\mathrm{d}\theta f^2=\pi R^2L. \tag{12}$$

It is trivial to verify that the cylinder, of volume $V = \pi R^2L$, is a solution of the equations listed above and complies with all boundary conditions. This solution is given by

$$f^0=R,$$
$$\Phi^0=\frac{U}{L}(z+\tfrac{1}{2}L),$$
$$\Delta p^0+\tfrac{1}{2}\Delta[\epsilon(1-b)]\left(\frac{U}{L}\right)^2+\frac{\sigma}{R}=0.$$

The set of equations is non-dimensionalized as follows: $\boldsymbol{r}=\boldsymbol{r}'R$, $p=p'\sigma/R$, $\Phi=\Phi'U$ and leads to an equivalent set for the primed quantities wherein three non-dimensional numbers appear. These numbers are $\Lambda\equiv L/2R$, which represents the 'slenderness' of the bridge; $\beta_0\equiv\epsilon_0/\epsilon_i$, i.e. the relative permittivity of the outer liquid with respect to the inner one (we also define $\beta_1\equiv\epsilon_i/\epsilon_i=1$), and $\Xi^2\equiv\epsilon_i U^2/\sigma R$, defined as the 'bifurcation parameter', which represents the ratio of electrical to superficial tension forces.

From here on we shall, for convenience, drop all primes.

3. Shape bifurcation and stability

The perfectly cylindrical liquid bridge is an equilibrium configuration for any value of the imposed external parameters (Λ,β_0,Ξ). Nevertheless, as we move through a critical two-dimensional surface in this three-dimensional parameter space, it happens that the cylinder loses its stability and another family branches off. Our immediate aim in this section is to determine this surface and thus delineate the instability region for the cylindrical solution. We deform the system about the equilibrium solution and now examine its behaviour as a function of the relevant parameters. The bifurcation surface comes from the condition that some other solution exists near the equilibrium:

$$f=f^0+\tilde{f},$$
$$\Phi=\Phi^0+\tilde{\phi},$$
$$\Pi_\alpha=\Pi_\alpha^0+\tilde{\pi}_\alpha \quad (\alpha=\mathrm{o},\mathrm{i}),$$

where the non-dimensionalized equilibrium solution is

$$f^0 = 1, \quad \Phi^0 = \frac{1}{2\Lambda}(z+\Lambda),$$
$$\Pi_o^0 = -\beta_o(1-b_o)\frac{\Xi^2}{8\Lambda^2}, \quad \Pi_i^0 = 1-\beta_i(1-b_i)\frac{\Xi^2}{8\Lambda^2}.$$

Assuming that the perturbations are small, linearization of (4) and conditions (5)–(8), and (10)–(12), gives, to first order

$$\nabla^2\tilde{\phi} = 0, \tag{13}$$

along with

$$\tilde{f}+\frac{\partial^2\tilde{f}}{\partial z^2}+\frac{\partial^2\tilde{f}}{\partial\theta^2} = \left[\Delta\tilde{\pi}+\tfrac{1}{2}\Delta\left(\beta\frac{\partial\tilde{\phi}}{\partial z}\right)\frac{\Xi^2}{\Lambda}\right]_{r=1}, \tag{14}$$

$$\frac{\Delta\beta}{2\Lambda}\frac{\partial\tilde{f}}{\partial z} = \left[\Delta\left(\beta\frac{\partial\tilde{\phi}}{\partial r}\right)\right]_{r=1}, \tag{15}$$

$$[\Delta\tilde{\phi}]_{r=1} = 0, \tag{16}$$

$$\tilde{\phi}(r,\theta,\pm\Lambda) = 0, \tag{17}$$

$$\tilde{\phi}(0,\theta,z) = \text{finite}, \tag{18}$$

$$\tilde{\phi}(\infty,\theta,z) = 0, \tag{19}$$

$$\tilde{f}(\theta,\pm\Lambda) = 0, \tag{20}$$

$$\int_{-\Lambda}^{\Lambda} dz \int_0^{2\pi} d\theta\tilde{f} = 0. \tag{21}$$

In order to solve Laplace's equation in both zones independently we use the classical separation of variables technique with conditions (16)–(19), giving the following sets of independent modes:

$$\left.\begin{aligned}\tilde{\phi}_{i,m}(r,z) &= \sum_{n=1}^{\infty} A_{nm}\frac{I_m(x_n r)}{I_m(x_n)}\sin[x_n(z+\Lambda)],\\ \tilde{\phi}_{o,m}(r,z) &= \sum_{n=1}^{\infty} A_{nm}\frac{K_m(x_n r)}{K_m(x_n)}\sin[x_n(z+\Lambda)],\end{aligned}\right\} \quad \text{for } m = 0, \pm1, \pm2, \ldots. \tag{22}$$

Here I_m and K_m are the modified Bessel functions of first and second kind; x_n is defined as $n\pi/2\Lambda$, and A_{nm} are constants to be found from the remaining conditions.

The general solution is then of the form

$$\tilde{\phi}(r,\theta,z) = \sum_{m=-\infty}^{\infty}\tilde{\phi}_m(r,z)\,e^{im\theta} \tag{23}$$

for the potential, and

$$\tilde{f}(\theta,z) = \sum_{m=-\infty}^{\infty}\tilde{f}_m(z)\,e^{im\theta} \tag{24}$$

for the interface, where we always consider the real part of the expressions only. The non-dependence of these modes comes from the linearity of the equations and boundary conditions.

From (14), (23) and (24), we have for each mode $\tilde{f}_m$:

$$\frac{d^2\tilde{f}_m}{dz^2}+(1-m^2)\tilde{f}_m = \Delta\tilde{\pi}\,\delta_{m0}+\frac{\Xi^2}{2\Lambda}\left[\Delta\left(\beta\frac{\partial\tilde{\phi}_m}{\partial z}\right)\right]_{r=1}, \tag{25}$$

where δ_{m0} is the Kronecker delta (1 for $m = 0$ and 0 otherwise). For distinct values of m (0, 1 and m arbitrary and greater than 1) we have the following solutions (here we assume that the right-hand side of (25) can be written in the form of a series of cosine terms):

$$\tilde{f}_0 = C_0 \sin z + D_0 \cos z + \sum_{n=1}^{\infty} a_{n0} \cos[x_n(z+\Lambda)] + \Delta\tilde{\pi}, \tag{26}$$

$$\tilde{f}_1 = C_1 z + D_1 + \sum_{n=1}^{\infty} a_{n1} \cos[x_n(z+\Lambda)], \tag{27}$$

$$\tilde{f}_m = C_m \sinh[(m^2-1)^{\frac{1}{2}} z] + D_m \cosh[(m^2-1)^{\frac{1}{2}} z] + \sum_{n=1}^{\infty} a_{nm} \cos[x_n(z+\Lambda)], \tag{28}$$

the last for $|m| > 1$. C_m, D_m and a_{nm} are arbitrary constants to be fixed from boundary conditions.

We may derive expressions for a_{nm} (for all n and m) as functions of A_{nm} by substituting (22) and (26)–(28) into (25), from which we deduce

$$a_{nm} = \frac{\Xi^2 \Delta\beta}{2\Lambda} \frac{x_n}{1-m^2-x_n^2} A_{nm}. \tag{29}$$

Analysis of the $m = 0$ mode

We shall study the particular case of axisymmetric perturbations, i.e. $m = 0$. First since we may write (26) as a function of the constants A_{n0} rather than a_{n0} we must evaluate those coefficients. To do this we split (15) into m-modes, giving a corresponding set of m equations which must be verified independently, and for that of $m = 0$ we substitute (22) and (26), where we have to expand $\sin z$ and $\cos z$ in Fourier series of the argument $x_n(z+\Lambda)$, i.e.

$$\sin z = \frac{2\cos\Lambda}{\Lambda} \sum_{\substack{n=1 \\ n\,\text{odd}}}^{\infty} \frac{\cos[x_n(z+\Lambda)]}{1-x_n^2},$$

$$\cos z = \frac{\sin\Lambda}{\Lambda}\left\{1 + 2 \sum_{\substack{n=2 \\ n\,\text{even}}}^{\infty} \frac{\cos[x_n(z+\Lambda)]}{1-x_n^2}\right\}.$$

This gives

$$A_{n0}\left[\frac{\Xi^2\Delta\beta}{2\Lambda}\frac{x_n}{1-x_n^2} + \frac{2\Lambda}{\Delta\beta} H_0(\beta_0, x_n)\right] = \begin{cases} -\dfrac{2\cos\Lambda}{\Lambda}\dfrac{C_0}{1-x_n^2} & (n \text{ odd}) \\ -\dfrac{2\sin\Lambda}{\Lambda}\dfrac{D_0}{1-x_n^2} & (n \text{ even}) \end{cases} \tag{30}$$

where the function $H_m(x, y)$ is defined as

$$H_m(x, y) \equiv x\frac{K_m'(y)}{K_m(y)} - \frac{I_m'(y)}{I_m(y)}. \tag{31}$$

The prime indicates derivation with respect to the argument.

Relation (30) determines the A_{n0} coefficients as functions of the integration constants of the homogeneous equation (associated to (25)) for $\tilde{f}_0$, C_0 and D_0. By substituting the A_{n0} into the expressions for a_{n0} and the result into (26) we get the form of $\tilde{f}_0$ in terms of these integration constants and $\Delta\tilde{\pi}$. Thus we have three unknown constants and three conditions not yet used, i.e. (20) and (21). Note that

(20) can be written for each mode, and that integration over θ in (21) gives a condition for $\tilde{f}_0$ only:

$$\int_{-\Lambda}^{\Lambda} \tilde{f}_0 \, dz = 0.$$

Eventually, we arrive at the linear homogeneous system

$$C_0 \sin \Lambda + D_0 \cos \Lambda + \sum_{n=1}^{\infty} (-1)^n a_{n0} + \Delta\tilde{\pi} = 0,$$

$$-C_0 \sin \Lambda + D_0 \cos \Lambda + \sum_{n=1}^{\infty} a_{n0} + \Delta\tilde{\pi} = 0,$$

$$D_0 \sin \Lambda + \Lambda \Delta\tilde{\pi} = 0.$$

After some manipulation we obtain the following conditions:

$$\Lambda \tan \Lambda + 2 \sum_{\substack{n=1 \\ n \text{ odd}}}^{\infty} \left\{ (1-x_n^2) \left[1 + \frac{4\Lambda^2 H_0(\beta_0, x_n)(1-x_n^2)}{\Xi^2 (\Delta\beta)^2 x_n} \right] \right\}^{-1} = 0, \tag{32}$$

$$1 - \Lambda \cot \Lambda + 2 \sum_{\substack{n=2 \\ n \text{ even}}}^{\infty} \left\{ (1-x_n^2) \left[1 + \frac{4\Lambda^2 H_0(\beta_0, x_n)(1-x_n^2)}{\Xi^2 (\Delta\beta)^2 x_n} \right] \right\}^{-1} = 0, \tag{33}$$

which relate in an implicit form the parameters Ξ, β_0 and Λ. For the case of zero applied voltage we are left with only the first terms in the two previous equations. This leads to the well-known solution given by Sanz (1985): (32) gives $\Lambda = \pi, 2\pi, \ldots$ while (33) gives $\Lambda = 4.49, 10.90, \ldots$, etc. It is well known that at the first bifurcation point, i.e. $\Lambda = \pi$, for no applied voltage, the cylindrical solution for the bridge is unstable. Once we apply a field the point $\Lambda = \pi$ expands to a surface in Ξ–β_0–Λ space. This is also true for each corresponding value of Λ in the two infinite series given above. Thus we end up with a discrete family of nested surfaces which do not intersect. An inviscid dynamical analysis shows that this first bifurcation surface (corresponding to $\Lambda = \pi$) is also where instability sets in (González *et al.* 1988). To plot this surface, shown on figure 2, we solved the equations using a Newton–Raphson type numerical method after accounting for the asymptotic behaviour of the series. The unstable region in Ξ–β_0–Λ space is that below the surface where all the other nested surfaces lie. Therefore the stability curve is given by (32). The conclusion to be drawn from this is that the bridge will always break asymmetrically about the central plane (parallel to the plates) since this equation is representative of odd modes of deformation. This agrees with experimental observation. The effect of varying β_0 is quite evident from this perspective graph. Clearly, when $\beta_0 = 1$, i.e. no difference in the permittivity of each non-conducting liquid, the applied voltage has no influence on stability and all bridges of slenderness $\Lambda > \pi$ are unstable. On the other hand, the larger the difference in permittivities of the two liquids (high or low values of β_0), the lower the field necessary to hold a given bridge is. For moderate values of β_0 (approaching 1) the field increases quite substantially.

It is worth noting that it is of little consequence which of the two liquids forms the bridge (that with higher or lower permittivity) since inverting the liquids (i.e. the relevant parameters in (32)) will give similar values for the stability parameter Ξ. Effectively, interchanging the liquids is equivalent mathematically to making the following change of variables: $\beta_0 \to 1/\beta_0$ and $\Xi \to \beta_0 \Xi$. Putting these into the

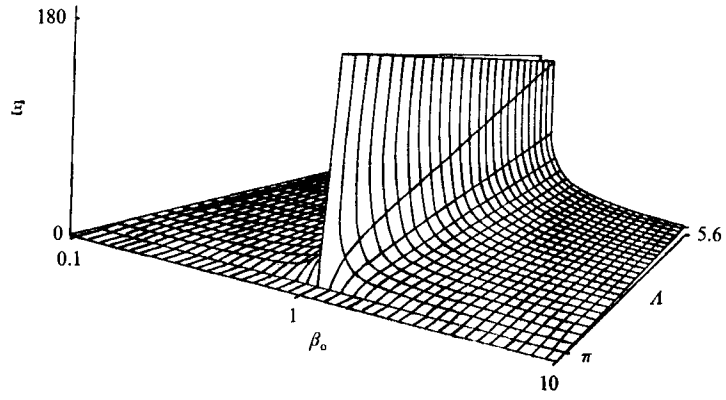

FIGURE 2. Perspective graph of the bifurcation surface in β_0–Λ–Ξ space corresponding to the first solution to (32). Above the surface is the stable zone. All other bifurcation surfaces (corresponding to the remaining solutions of (32) and all solutions of (33)) lie below this one. Note that the β_0-axis is of logarithmic scale.

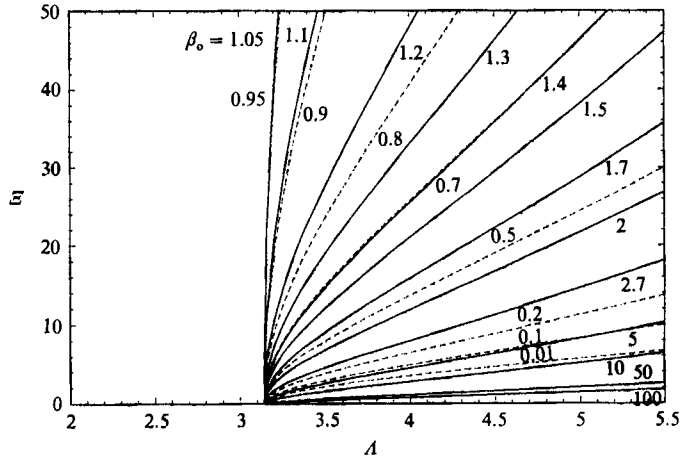

FIGURE 3. Graph in Ξ–Λ space of the stability curves for a set of different β_0 values: solid lines, $\beta_0 > 1$; broken lines, $\beta_0 < 1$.

governing equations and boundary conditions, the only modification is that $H_m(x, y)$ is replaced by $H_m^*(x, y)$ given by

$$H_m^*(x, y) \equiv \frac{K_m'(y)}{K_m(y)} - x\frac{I_m'(y)}{I_m(y)}.$$

This function takes values close to those of $H_m(x, y)$.

From the definition of the electrical stability parameter Ξ we can see the influence of the interfacial tension. With Ξ^2 proportional to the inverse of σ, it is obvious that as σ increases, the stabilizing field also increases. This is in contrast to the zero applied field case where interfacial tension does not intervene in the stability criterion.

To illustrate further the nature of the bifurcation and to present a more quantitative aspect, we show a series of stability curves in Ξ–Λ space for a number of different values of β_0 (figure 3). Thus for any two given fluids, corresponding to one value of β_0 and thus one curve on the graph, the curve can be used to estimate with some precision the value of the applied field necessary to hold stable a bridge of any

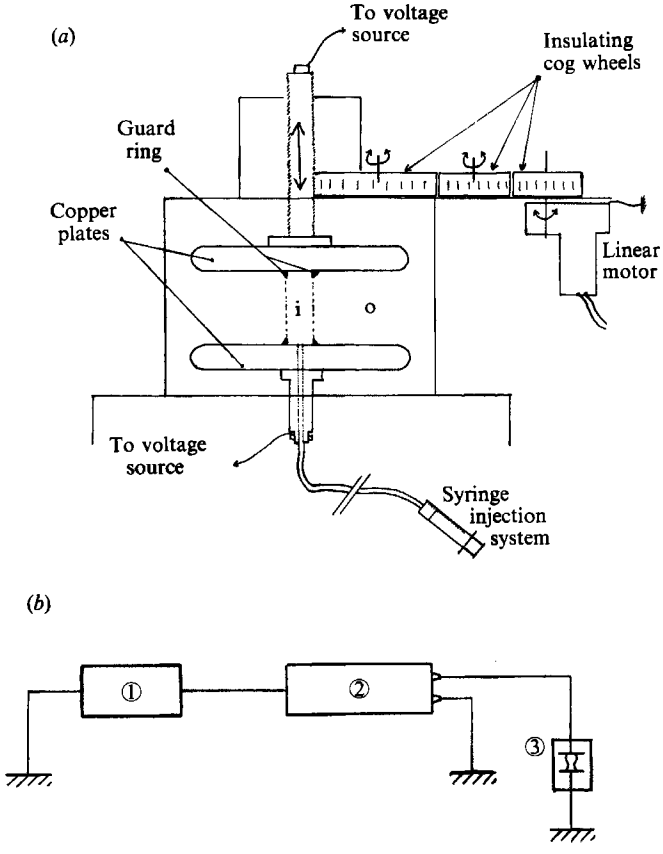

FIGURE 4. (a) Representation of the experimental cell. (b) Schematic of electrical circuit: (1) autotransformer (0–245 V); (2) transformer (220–20000 V); (3) experimental cell.

given length. In our case we verified this via comparison of experimental results to the theoretical curve with $\beta_0 = 0.55$ (see §4).

Finally, there is no static solution for the non-axisymmetric modes, $m > 0$ (see the Appendix). Non-axisymmetric dynamical modes were shown to be stable via a similar analysis to the axisymmetric case following a study of the resulting stability equations (González *et al.* 1988). This is not surprising in view of the general stabilizing effect of tangential electric fields.

4. Experimental results and discussion

The experimental cell is schematized in figure 4(a). The Plateau tank is made of Plexiglas ($10 \times 10 \times 10$ cm^3) and the two electrodes of copper (electrode diameter: 8 cm). These last are 5 mm thick with rounded edges in order to decrease field distortion effects. Small copper or nylon guard (or containing) rings, 5 mm in diameter, were glued to the centre of each electrode. These were used to anchor the bridge at well-defined boundaries. With such large parallel flat electrodes we could be reasonably sure of having a parallel field tangential to the liquid bridge and in the axial direction. The upper electrode was vertically mobile and the maximum electrode gap was 5 cm.

	Dielectric constant	Density at 25 °C (kg/m³)	Electrical conductivity (S/m)	Interfacial tension (mN/m)
Silicone oil	2.6	957	$\sim 10^{-13}$	8.4
Ricinus oil	4.76	957	2.5×10^{-10}	

TABLE 1. Physical properties of the liquids: silicone oil, outer; ricinus oil, inner

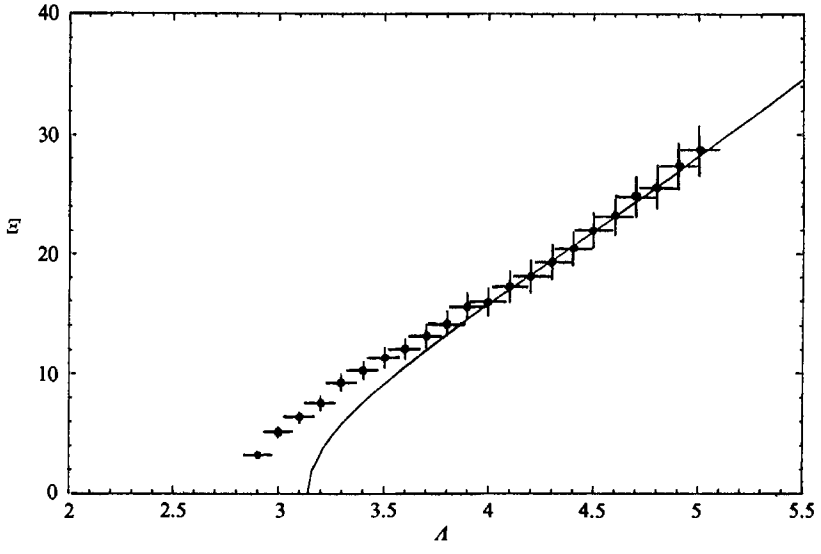

FIGURE 5. Comparison between experimental points and the theoretical curve corresponding to $\beta_0 = 0.55$. The magnitudes of the error bars are discussed in the text.

The lower electrode was fixed and had a small hole in its centre through which liquid injection or extraction could be carried out. We used an insulin syringe attached to a thin transparent nylon tube in order to measure the volume of liquid injected into the bridge. Thus, knowing the height, diameter and the rate of opening of the electrode gap, we could ensure that the liquid bridge volume corresponded to that of a cylinder of equal dimensions.

The upper electrode was driven by a 15 V d.c. linear motor attached to a set of insulating cog wheels. The vertical velocity of the electrode had a maximum of 2 mm/min. The metal supporting shaft was encased in a nylon cylinder to ensure adequate electrical insulation. The two leads from the a.c. voltage source were connected to the supporting shafts of each electrode.

The liquids used were silicone oil (Rhodorsil 47V50) and ricinus oil. Some of the relevant physical properties of these liquids are given on table 1. The ricinus oil was injected to form the bridge with the silicone as the surrounding liquid. This configuration was chosen since the latter had a lower conductivity and is completely transparent, facilitating visualization.

The electrical circuit is schematized in figure 4(*b*). An auto-transformer (output: 0–245 V, 160 VA.) fed an a.c. transformer (220–20000 V), the outputs of which went to each electrode. The circuit operated at industrial frequency (50 Hz).

The operating method was to first form a small bridge and then apply the electric field. Thus stabilized, the electrode gap was slowly opened and enough liquid injected

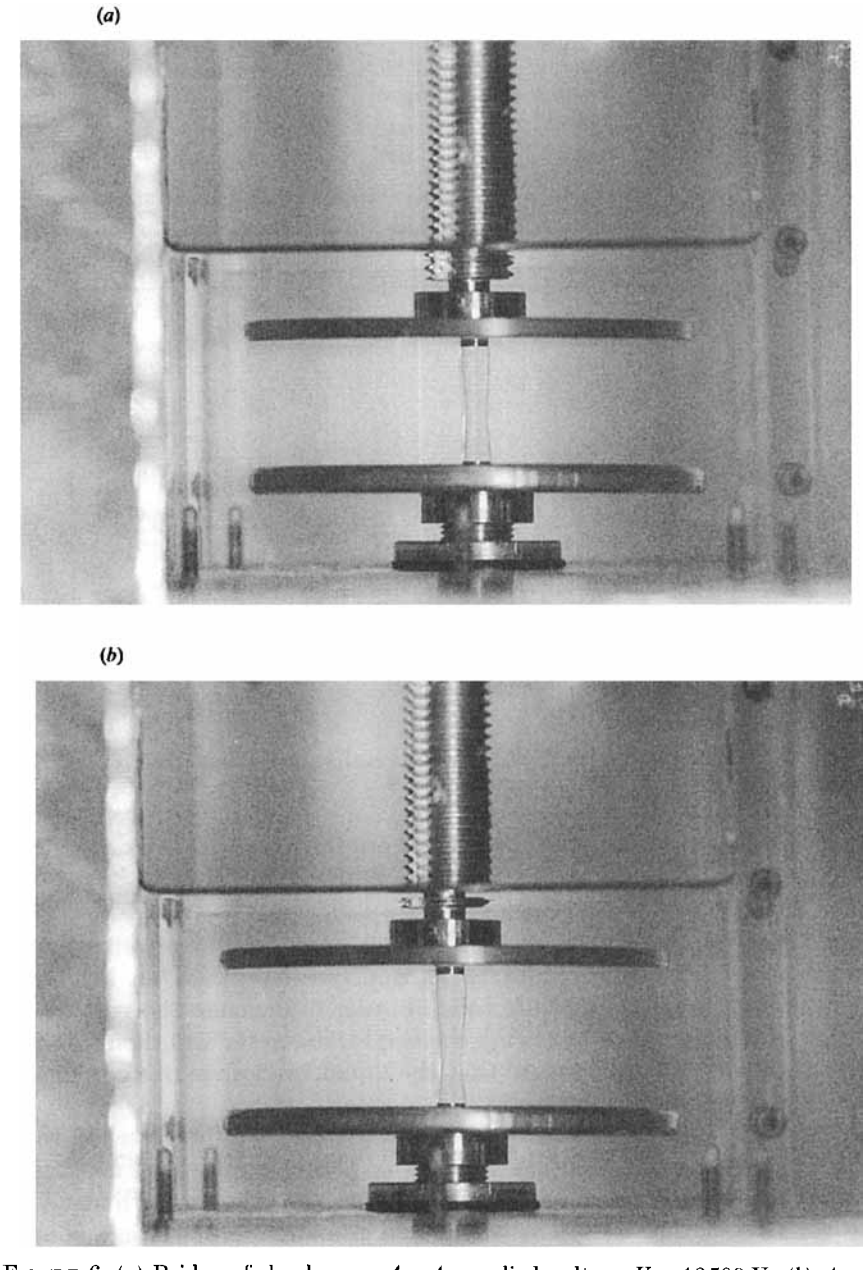

FIGURE 6. (*a*) Bridge of slenderness $\Lambda = 4$; applied voltage $V = 16500$ V; (*b*) $\Lambda = 5$, $V = 21000$ V.

to keep the 'cylindrical volume'. Then, for a given height, we gradually decreased the electrical field until the bridge broke. This was verified by numerous repetitions of the experiment. The ambient temperature was always close to 25.5 °C.

In order to compare the experimental curve with the theoretical (figure 5) ones, we had to experimentally evaluate the surface tension between the ricinus and silicone oils, a proper evaluation of which is not, to our knowledge, available in the literature. We evaluated it as being equal to 8.4 mN/m (to within an error of about 10% in our experimental conditions), using the method given by Sanz (1985).

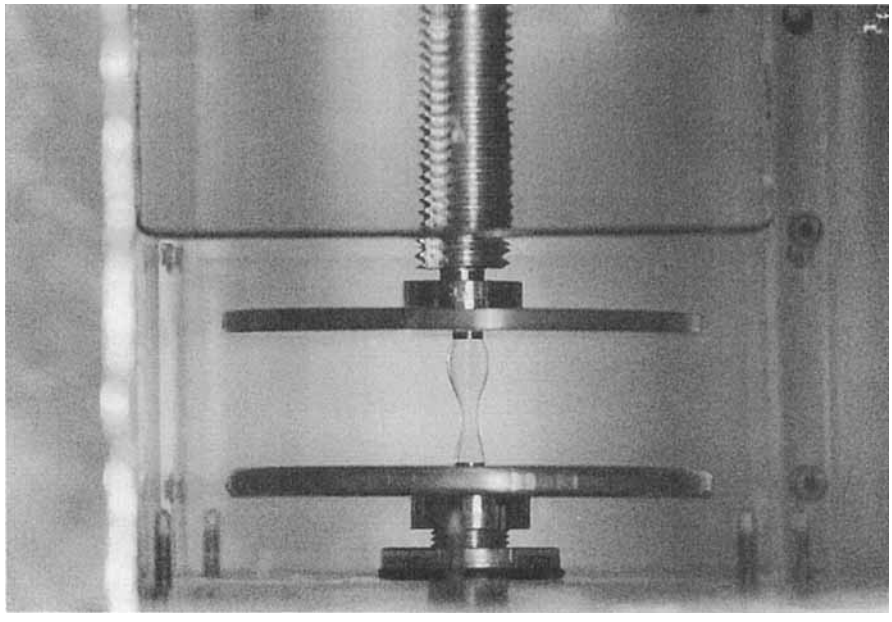

FIGURE 7. Bridge in process of breaking ($\Lambda = 4$, $V = 0$).

Further sources of possible experimental error include the exact values of the applied voltage (input voltage and multiplication factor), the radius of the bridge, its height and liquid volume and the value of the dielectric constant of the inner fluid. First, concerning the slenderness, we estimate the relative error to be 2.4%, taking into account possible maximum errors in the diameter of the bridge, its volume and its height. For the parameter Ξ, we estimated in the usual way the errors in interfacial tension, bridge radius and voltage from the autotransformer. Regarding the conversion factor of the transformer and the permittivities of the liquids we took the imprecision in the values supplied by the manufacturers to be 1%. Thus we calculated a total relative error of some 9%. The major source of imprecision is due to the interfacial tension evaluation (responsible for more than half). Note that all error bars are taken for the most unfavourable conditions.

On figure 5 are given the experimental values and the theoretical curve of Ξ as a function of Λ for the corresponding value of β_0. Agreement between them is quite satisfactory. The significant difference for values close to $\Lambda = 2.8$ should be expected since the effect of gravity, due to the small differences in liquid density, becomes important for small values of the applied electric field. As was suggested by one of the referees, an 'effective' value of the slenderness equal to 2.8 instead of π is obtained if one assumes a difference in liquid densities of 2 Kg/m^3 (Rivas & Meseguer 1984). The results of this series of experiments serve to verify the theoretical analysis both qualitatively and quantitatively.

From the photographs we see stable bridges of different slenderness greater than π. The bridges shown in figures 6(*a*) and 6(*b*) are of slendernesses 4 and 5 respectively. Both of these are stable in time. The applied voltage for the first is 16500 V, well above the critical voltage for this bridge, and hence it is almost symmetrical through the central plane. For the second, we see that the bridge has a more pronounced amphoric shape, since the voltage is quite close to the critical one ($V = 21$ kV $>$ $V_c = 10.4$ kV). The bridge will not be cylindrical since the Bond number ($\Delta\rho g R^2/\sigma$)

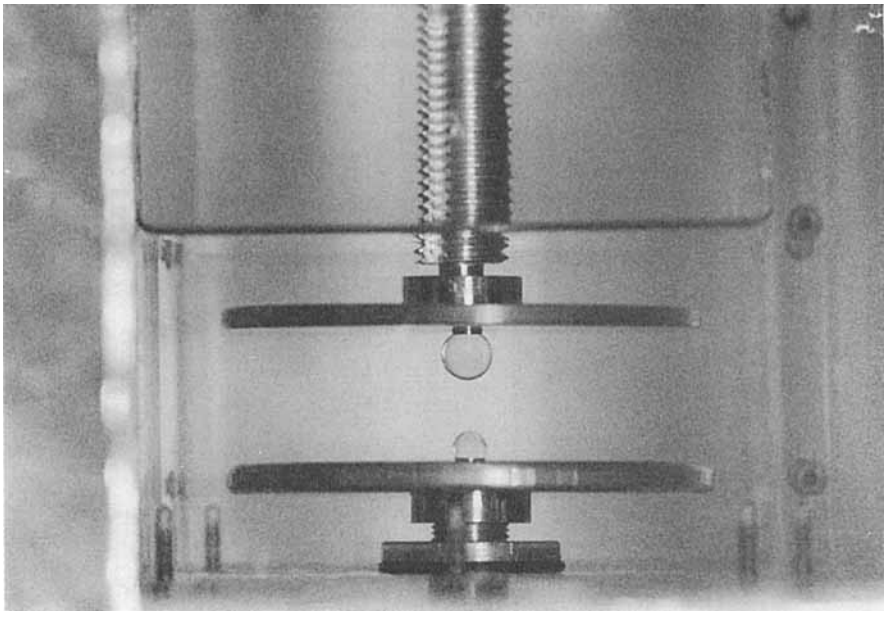

FIGURE 8. The bridge broken asymmetrically into two drops and a central satellite.

is not exactly zero. In figure 7, a bridge of slenderness 4 is shown as the field is cut off. We can clearly see the non-symmetric way in which this happens both here and in figure 8 where the volume of one drop is evidently larger than the other.

5. Conclusion

The effect of an applied a.c. electric field on a liquid bridge (of non-conducting liquids) is to stabilize it if there is a difference in dielectric constant values between the two fluids involved. It does not appear to matter which liquid of the two forms the bridge, that of higher or lower permittivity. As the difference in dielectric constant between the liquids increases, the electric field necessary to hold a given bridge decreases. Increasing the interfacial tension has a similar effect.

The above points where possible were verified experimentally with good agreement found between theory and experiment.

As a final remark, we consider that the stabilizing influence of the electric field could be useful in the processing of non-conducting materials. Nevertheless, further research is necessary in order to characterize the interplay between these electrical effects and thermal gradients along the liquid bridge.

This research has been partially supported by the Consejería de Educación de la Junta de Andalucía, and was conducted at the Universidad de Seville (Spain) in partial fulfilment of the requirements for the doctoral degree of one of the authors (H.G.) One of the authors (F.M.J.McC.) benefited from a CAICYT postdoctoral fellowship. We also wish to acknowledge fruitful discussions with Professor M. G. Velarde of the UNED (Madrid).

Appendix. Demonstration of stability of non-axisymmetric modes

Mode $|m| = 1$

For $|m| = 1$ we must make use of (27), where the a_{n1} are given by (29), with the appropriate value of m. The function z in (27) is written as a Fourier (cosine) series:

$$z = -\frac{2}{\Lambda} \sum_{\substack{n=1 \\ n\,\text{odd}}}^{\infty} \frac{\cos[x_n(z+\Lambda)]}{x_n^2}$$

and the resulting expression for $\tilde{f}_1$ is substituted, as in the text, into (15), for $m = 1$. We then obtain the following expression for a_{n1} as a function of C_1, using (29):

$$a_{n1} = \begin{cases} -\dfrac{2C_1}{\Lambda}\left[1 - \dfrac{4\Lambda^2 x_n H_1(\beta_0, x_n)}{\Xi^2(\Delta\beta)^2}\right]^{-1} & (n \text{ odd}), \\ 0 & (n \text{ even}). \end{cases}$$

Of the three conditions that we have for $\tilde{f}_0(z)$ (the anchor conditions and that of constant volume), we retain the first two:

$$\tilde{f}_1(\pm\Lambda) = 0.$$

From these we obtain that $C_2 = 0$ and the condition

$$C_1\left[1 + \sum_{\substack{n=1 \\ n\,\text{odd}}}^{\infty} \left(1 - \frac{4\Lambda^2 x_n H_1(\beta_0, x_n)}{\Xi^2(\Delta\beta)^2}\right)^{-1}\right] = 0.$$

Since $H_1(\beta_0, x_n)$ is always negative, the expression in parentheses is always positive and we deduce that $C_1 = 0$. Clearly, $\tilde{f}_1(z) = 0$ also. That is to say that the only solution is the trivial one and that this mode is stable for all values of Λ, β_0 and Ξ.

Modes $|m| > 1$

Here we use conditions (32) and (33), with the expressions in series:

$$\sinh[(m^2-1)^{\frac{1}{2}}z] = -\frac{2(m^2-1)^{\frac{1}{2}}\cosh[(m^2-1)^{\frac{1}{2}}\Lambda]}{\Lambda} \sum_{\substack{n=1 \\ n\,\text{odd}}}^{\infty} \frac{\cos[x_n(z+\Lambda)]}{x_n^2+m^2-1},$$

$$\cosh[(m^2-1)^{\frac{1}{2}}z] = \frac{(m^2-1)^{\frac{1}{2}}\sinh[(m^2-1)^{\frac{1}{2}}\Lambda]}{\Lambda}\left[\frac{1}{m^2-1} + 2\sum_{\substack{n=2 \\ n\,\text{even}}}^{\infty} \frac{\cos[x_n(z+\Lambda)]}{x_n^2+m^2-1}\right].$$

Proceeding in an analogous manner to the cases for $m = 0$ and $|m| = 1$, we obtain the following conditions for the coefficients C_m and D_m:

$$C_m\, Q_c(m, \Lambda, \beta, \Xi^2) = 0, \quad D_m\, Q_d(m, \Lambda, \beta, \Xi^2) = 0,$$

where

$$Q_c(m, \Lambda, \beta, \Xi^2) \equiv \Lambda \tanh[(m^2-1)^{\frac{1}{2}}\Lambda] - 2(m^2-1)^{\frac{1}{2}} \sum_{\substack{n=1 \\ n\,\text{odd}}}^{\infty} \left\{(x_n^2+m^2-1)\left[1 - \frac{4\Lambda^2 H_m(\beta_0, x_n)(x_n^2+m^2-1)}{\Xi^2(\Delta\beta)^2 x_n}\right]\right\}^{-1},$$

$$Q_d(m,\Lambda,\beta,\Xi^2) \equiv \Lambda\coth[(m^2-1)^{\frac{1}{2}}\Lambda] - 2(m^2-1)^{\frac{1}{2}}\sum_{\substack{n=2\\ n\,\text{even}}}^{\infty}\left\{(x_n^2+m^2-1)\left[1-\frac{4\Lambda^2 H_m(\beta_0,x_n)(x_n^2+m^2-1)}{\Xi^2(\Delta\beta)^2 x_n}\right]\right\}^{-1},$$

and $H_m(\beta,x_n)$ is defined in (31).

To demonstrate that $C_m = D_m = 0$, we need to prove that for any finite values of the parameters the expressions in curly brackets are non-zero. Thus the only solution is the trivial one and the modes $|m| > 1$ are stable. Let us therefore analyse the terms of the summation. Note that the expression

$$\left[1-\frac{4\Lambda^2 H_m(\beta_0,x_n)(x_n^2+m^2-1)}{\Xi^2(\Delta\beta)^2 x_n}\right]^{-1}$$

is a bounded quantity within the interval $[0,1]$, for all positive values of the parameters, since $H_m(\beta_0,x_n)$ is always negative and $x_n^2+m^2-1$ is positive for $|m| > 1$. Thus, the summation has a value bounded between zero and

$$\sum_{\substack{n=1\\ n\,\text{odd}}}^{\infty}(x_n^2+m^2-1)^{-1} \quad \text{for } Q_c$$

and zero and

$$\sum_{\substack{n=2\\ n\,\text{even}}}^{\infty}(x_n^2+m^2-1)^{-1} \quad \text{for } Q_d.$$

Thus

$$Q_c(m,\Lambda,\beta,\Xi^2) > \Lambda\tanh[(m^2-1)^{\frac{1}{2}}\Lambda] - 2(m^2-1)^{\frac{1}{2}}\sum_{\substack{n=1\\ n\,\text{odd}}}^{\infty}(x_n^2+m^2-1)^{-1} = 0$$

and

$$Q_d(m,\Lambda,\beta,\Xi^2) > \Lambda\coth[(m^2-1)^{\frac{1}{2}}\Lambda] - 2(m^2-1)^{\frac{1}{2}}\sum_{\substack{n=2\\ n\,\text{even}}}^{\infty}(x_n^2+m^2-1)^{-1} = \frac{1}{\Lambda(m^2-1)^{\frac{1}{2}}} > 0.$$

The inequality is clear once the functions $\tanh x$ and $\coth x$ are developed in series of simple fractions (see for example Gradshteyn & Ryzhik 1980).

REFERENCES

Cheng, K. J. & Chaddock, J. B. 1984 Deformation and stability of drops and bubbles in an electric field. *Phys. Lett.* **A 106**, 51–53.

Denat. A., Gosse, B. & Gosse, J. P. 1979 Ion injections in hydrocarbons. *J. Electrostat.* **7**, 205–225.

González, H., Castellanos, A., McCluskey, F. M. J. & Gañan, A. 1988 Small oscillations of liquid bridges subjected to a.c. electric fields. In *Synergetics, Order and Chaos*. World Scientific (in press).

Gradshteyn, I. S. & Ryzhik, I. M. 1980 *Table of Integrals, Series, and Products*. Academic.

Hurle, D. T. J., Müller, G. & Nitsche, R. 1987 Cristal growth from the melt. In *Fluid Science and Materials Sciences in Space*, chap. X. Springer.

Landau, L. M. & Lifshitz, E. M. 1971 *Electrodynamics of Continuous Media*. Addison-Wesley.

Martínez, I., Haynes, J. M. & Langbein, D. 1987 *Fluid Statics and Capillarity*. In *Fluid Science and Materials Sciences in Space*, chap. II. Springer.

Melcher, J. R. 1963 *Field-Coupled Surface Waves*. M.I.T. Press.

MELCHER, J. R. & HURWITZ, M. 1967 Gradient stabilization of electrohydrodynamically oriented liquids. *J. Spacecraft Rockets* **4**, 864–871.

MELCHER, J. R. & SCHWARZ, W. J. 1968 Interfacial relaxation overstability in a tangential electric field. *Phys. Fluids* **11**, 2604–2616.

MIKSIS, M. J. 1981 Shape of a drop in an electric field. *Phys. Fluids* **24**, 1967–1972.

NAYYAR, N. K. & MURTY, G. S. 1960 The stability of a dielectric liquid jet in the presence of a longitudinal electric field. *Proc. Phys. Soc. Lond.* **75**, 369–373.

RIVAS, D. & MESEGUER, J. 1984 One-dimensional self-similar solution of the dynamics of axisymmetric slender liquid bridges. *J. Fluid Mech.* **138**, 417–429.

ROSENKILDE, C. E. 1969 A dielectric fluid drop in an electric field. *Proc. R. Soc. Lond.* A **312**, 473–494.

SANZ, A. 1985 The influence of an outer bath in the dynamics of axisymmetric liquid bridges. *J. Fluid Mech.* **156**, 101–140.

SAVILLE, D. A. 1970 Electrohydrodynamic stability: fluid cylinders in longitudinal electric fields. *Phys. Fluids* **13**, 2987–2994.

STRUIK, D. J. 1957 *Classical Differential Geometry*. Addison-Wesley.